

# Influence of silicon-nanocrystal distribution in $\text{SiO}_2$ matrix on charge injection and charge decay

Cite as: Appl. Phys. Lett. **86**, 152110 (2005); <https://doi.org/10.1063/1.1901831>

Submitted: 07 October 2004 . Accepted: 15 March 2005 . Published Online: 07 April 2005

C. Y. Ng, T. P. Chen, M. S. Tse, V. S. W. Lim, S. Fung, and Ampere A. Tseng



View Online



Export Citation



**Lake Shore**  
CRYOTRONICS

**8600 Series VSM**

For fast, highly sensitive measurement performance

[LEARN MORE](#) ▶

2017  
**R&D 100**  
WINNER

## Influence of silicon-nanocrystal distribution in SiO<sub>2</sub> matrix on charge injection and charge decay

C. Y. Ng, T. P. Chen,<sup>a)</sup> and M. S. Tse

*School of Electrical and Electronic Engineering, Nanyang Technological University, Singapore 639798, Singapore*

V. S. W. Lim

*Institute of Microelectronics, 11 Science Park Road, Singapore 117685, Singapore*

S. Fung

*Department of Physics, The University of Hong Kong, Hong Kong*

Ampere A. Tseng

*Department of Mechanical and Aerospace Engineering, Center for Solid State Electronics, Arizona State University, Arizona 85287-6106*

(Received 7 October 2004; accepted 15 March 2005; published online 7 April 2005)

Influence of distribution of silicon nanocrystals (nc-Si) embedded in SiO<sub>2</sub> matrix on charge injection and charge decay of the nc-Si has been investigated with electrostatic force microscopy. For nc-Si distributing in the surface region, the size of charge cloud does not change with decay time, and neighboring charges have no influence on the charge decay. In contrast, for nc-Si distributing away from the surface, the size linearly increases with decay time, and the neighboring charges can either accelerate or resist the charge decay depending on their charge signs. In addition, the characteristic decay time for the first distribution is much shorter than that for the second distribution. These results provide an insight into the dissipation mechanism of the charges stored in the nc-Si. © 2005 American Institute of Physics. [DOI: 10.1063/1.1901831]

Silicon nanocrystals (nc-Si) embedded in a SiO<sub>2</sub> matrix have attracted much attention due to their outstanding properties for the applications in optoelectronic and memory devices.<sup>1-7</sup> To utilize the nc-Si as a storage medium, a good understanding on its charge storage and decay characteristics is necessary. Usually, monitoring the charge decay characteristic is done by determining the flatband voltage shift from capacitance-voltage (*C-V*) measurement.<sup>7</sup> However, this technique provides only macroscopic device information as *C-V* measurement responses to only an average variation over a large area. There are few studies on the charging/discharging behaviors of nc-Si at the level of nanometer scale. Recently, studies on charge storage of silicon nanocrystals,<sup>8-11</sup> Co nanocrystals,<sup>12</sup> silver nanocrystals<sup>13</sup> and CdSe nanocrystals<sup>14</sup> in SiO<sub>2</sub> film by using atomic force microscopy (AFM)/electrostatic force microscopy (EFM) have been reported. In this letter, we present a study on the influence of nc-Si distribution in a SiO<sub>2</sub> matrix on the charge injection and charge decay characteristics of the nc-Si using the EFM technique. Such a study should be very useful to memory application of the nc-Si.

SiO<sub>2</sub> films were thermally grown to 750 nm on either *p*-type or *n*-type (100) oriented Si wafers in dry oxygen at 950 °C. Si<sup>+</sup> ions with a dose of  $3 \times 10^{16}$  cm<sup>-2</sup> were then implanted to the SiO<sub>2</sub> thin films at 10 keV (sample X) and 14 keV (sample A). Thermal annealing was carried out at 1000 °C in N<sub>2</sub> ambient for 1 h to induce nc-Si formation. After annealing, for sample A about 17 nm SiO<sub>2</sub> was removed in diluted HF solution. The peak concentration of nc-Si is located very close to the SiO<sub>2</sub> surface for sample A and at the depth of ~16 nm underneath the surface for

sample X. Transmission electron microscopy (TEM) measurement indicates that the mean size of nc-Si for both samples is ~4 nm. EFM studies were performed at room temperature in air with a Veeco/Digital Instrument Dimension 3000 Scanning Probe Microscope. Charge was injected to the sample via the contact-mode EFM, while the tapping-mode EFM was used to monitor the discharging of nc-Si. The total charge stored in the nc-Si can be mapped with the EFM based on the total force acting on the EFM tip due to the Coulomb interaction between the sample surface and the tip.<sup>8,12</sup>

To inject charge into the samples, the EFM tip is touching the sample surface. For sample X, most of the nanocrystals distribute in the region of ~5–30 nm underneath the SiO<sub>2</sub> surface. To inject charges into these nanocrystals, the charges need to overcome the barrier of SiO<sub>2</sub> with a distance of at least 5 nm. In contrast, for sample A, most of the nanocrystals distribute from the surface to a depth of ~20 nm with its peak concentration located very close to the surface, and thus charge injection is much easier to occur. Therefore, for a given charge injection time, the injected charge number of sample A should be larger than that of sample X. As the injected charges will diffuse into neighboring uncharged nc-Si, the size of the injected charge cloud of sample A should also be larger than that of sample X. We have measured the number of the injected charges and the size of the charge cloud with EFM after the injection at -4 V for 10 s. Note, that it takes 3 min to complete an EFM snap shot after the charge injection. Therefore, it is impossible to determine the injected charge and the size of the charge cloud at the time of the completion of the injection due to the time required for setting up the measurement. However, based on the decay time dependence of the size of charge cloud and

<sup>a)</sup>Electronic mail: echentp@ntu.edu.sg

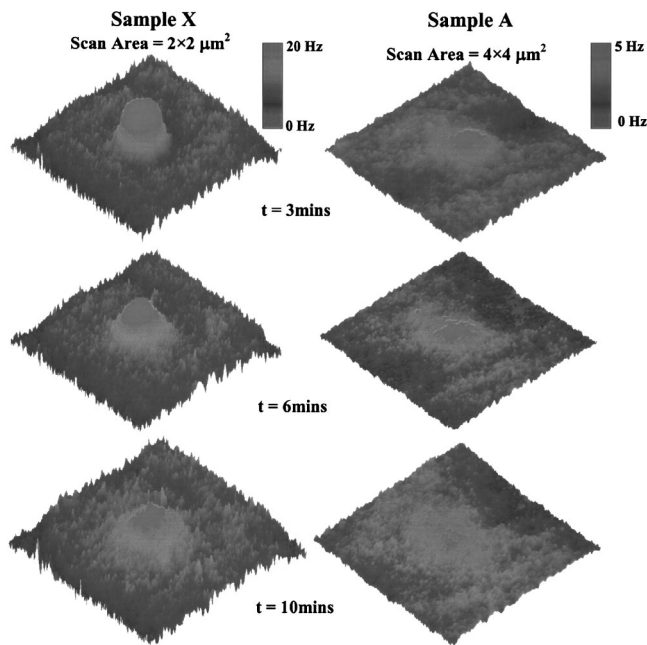


FIG. 1. 3D EFM images taken at various time after charge injection for sample A and sample X.

the number of trapped charge, we have been able to estimate the number of injected charge and the initial size of the charge cloud. The numbers of injected charges are  $\sim 84$  and  $\sim 1103$  electrons for sample X and sample A, respectively; and the sizes of the charge clouds are  $\sim 0.54 \mu\text{m}$  and  $\sim 1.25 \mu\text{m}$  for sample X and sample A, respectively. The details on the determination of the charge number and the charge cloud size are given below.

Figure 1 shows the 3D EFM images of samples X and A as a function of decay time after the injection at  $-4 \text{ V}$  for 10 s. The size (i.e., the diameter) of charge cloud can be determined from pseudo-Voigt fitting to the shift of the resonance frequency versus the position obtained from the EFM measurement based on 10% of the peak height, as shown in Fig. 2(a). The decay time dependence of the size of the charge cloud for the two samples is shown in Fig. 2(b). For sample A, the size of the charge cloud does not change with the decay time and is  $\sim 1.25 \mu\text{m}$  for decay time longer than 3 min. Therefore, the initial size of the charge cloud (i.e., when decay time=0) is expected to be  $\sim 1.25 \mu\text{m}$ . For sample X, the size of charge cloud increases with the decay time linearly. The linear relationship indicates that the speed of the lateral charge diffusion is constant. The initial size of the charge cloud for sample X can be estimated from the linear relationship with decay time=0, and it is  $0.54 \mu\text{m}$  as mentioned earlier. The influence of the nc-Si distribution on the size of charge cloud can be clearly seen in Fig. 2(b). The size for sample X is smaller than that for sample A. However, it increases with decay time linearly. In contrast, the size for sample A does not change with decay time. These results are explained in the following. For sample A with most of the nanocrystals distributing in the surface region, lateral charge diffusion occurs easily during the charge injection, leading to a larger charge cloud; however, after the injection, there is no more lateral diffusion as the injected charges can easily dissipate on the surface, and thus the size of the charge cloud remains unchanged during the decay period. For sample X with most of the nanocrystals distributing in the region at

least  $\sim 5 \text{ nm}$  away from the surface, the charge injection is relatively difficult, and thus the charge cloud is smaller; after the injection, the injected charges diffuse in all directions, leading to the increase in the size of the charge cloud with decay time.

Figure 3 shows the charge decay characteristics for sample X and sample A after the injection at  $-4 \text{ V}$  for 10 s. As shown in Fig. 3, the charge decay follows an exponential law, i.e.,  $Q(t) = Q_0 \exp(-t/\tau)$  where  $Q_0$  is the initial charge (i.e., the injected charge),  $\tau$  is the characteristic decay time and  $t$  is the time after charge injection. The fitting to the experimental data of charge versus decay time with the exponential law yields the initial charge ( $Q_0$ ) and the characteristic decay time ( $\tau$ ). The initial charge is 84 electrons for sample X and 1103 electrons for sample A, while the characteristic decay time is 310 s for sample X and 155 s for sample A. The initial charge of sample A is much larger than that of sample X, indicating that the charge injection into sample A is easier and more efficient; however, the characteristic decay time of sample A is shorter than that of sample X, which can be explained by the easy charge dissipation on the surface of sample A. The reason for these results is that in sample A, the existence of a large amount of nc-Si in the surface region made the charge injection easier, and exposing

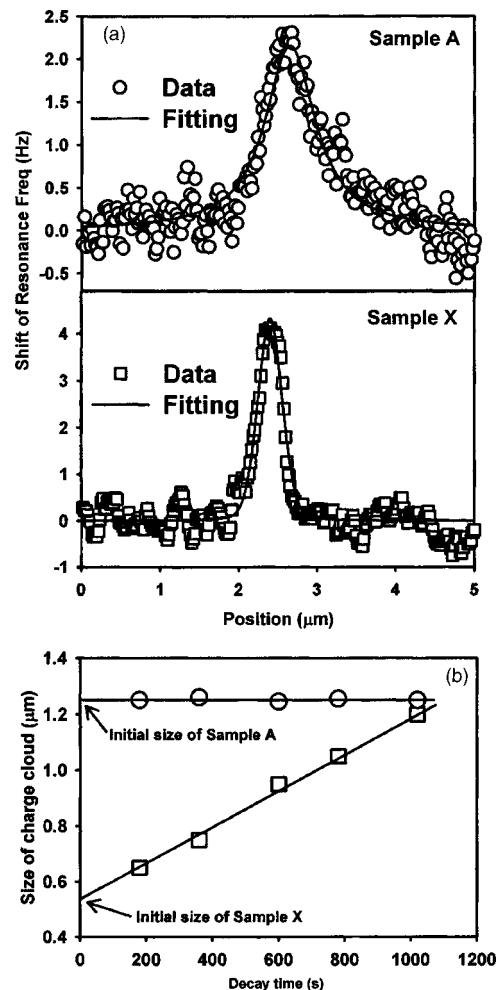


FIG. 2. (a) Determination of the size of charge cloud from the pseudo-Voigt fittings to the experimental data of the resonance-frequency shift vs position; and (b) size of charge cloud as a function of decay time. The charge injection is carried out at  $-4 \text{ V}$  for 10 s. The initial size just after charge injection can be obtained from the extrapolation to 0 s of decay time.

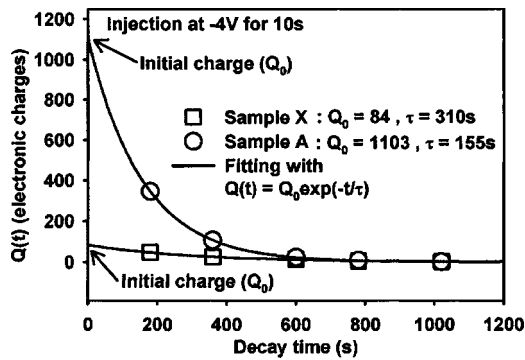


FIG. 3. Charge decay characteristics for sample X and sample A. The initial charge ( $Q_0$ ) and the characteristic decay time ( $\tau$ ) can be obtained from the fitting based on  $Q(t) = Q_0 \exp(-t/\tau)$ .

the nc-Si in air (i.e., humid environment) speeded up the charge dissipation. These results are consistent with the above discussions on the sizes of the charge clouds.

The charge decay could be affected by neighboring charges. To study the influence of neighboring charges, we have created one additional charge cloud close to the charge cloud under test (i.e., the EFM measurement is conducted on this charge cloud). The charge cloud under test is negative and is formed by the charge injection at  $-4$  V for 10 s; while the additional charge cloud is either negative or positive and is formed by the charge injection at  $-4$  V or  $+4$  V for 10 s, respectively. As pointed out earlier, the initial size of the charge cloud under test just after the charge injection are  $\sim 1.25 \mu\text{m}$  and  $\sim 0.54 \mu\text{m}$  for sample A and sample X, respectively. Therefore, the center of the additional charge cloud is set to locate  $\sim 1 \mu\text{m}$  and  $\sim 0.3 \mu\text{m}$  away from the center of the charge cloud under test for sample A and sample X, respectively. Note, that the time interval between the end of charge injection of the charge cloud under test and the start of the charge injection of the additional charge cloud is  $\sim 2$  s, which is too short to have a significant impact on the decay study. The influence of the neighboring charges on the characteristic decay time is shown in Fig. 4. For sample X, a negative or positive neighboring charge leads to a longer or shorter characteristic decay time, respectively. This means that the negative neighboring charge resists the charge dissipation of the negative charge cloud under test while the positive neighboring charge accelerates the charge dissipation. However, for sample A, the neighboring charges have no significant influence on the charge decay. The difference between the two samples is consistent with the early discussions on the influence of the nc-Si distribution on the charge diffusion. For sample A, as mentioned early there is no lateral charge diffusion during the decay period because the injected charges can easily dissipate on the surface, and therefore the neighboring charges have no significant influence on the charge decay. For sample X, there is a strong lateral charge diffusion during the decay period. As the neighboring charges can either accelerate or resist the lateral charge diffusion, they have a significant influence on the charge decay.

In summary, charge injection and charge decay are seriously affected by the distribution of the nc-Si in the  $\text{SiO}_2$

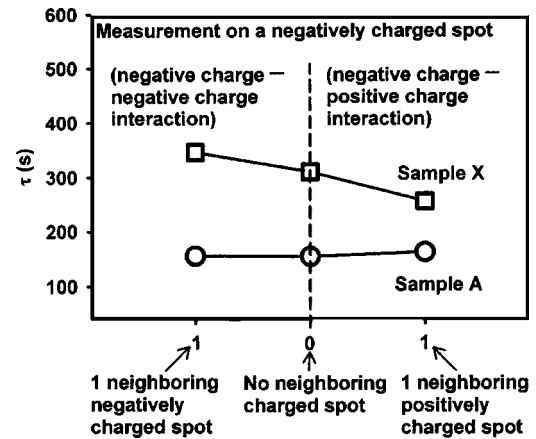


FIG. 4. Influence of neighboring charge on the characteristic decay time.

film, which is very important to the memory application of the nc-Si. For nc-Si distributing in the surface region, the size of charge cloud does not change with decay time, and neighboring charges have no influence on the charge decay. In contrast, for nc-Si distributing away from the surface, the size linearly increases with decay time, and the neighboring charges can either accelerate or resist the charge decay depending on their charge signs. In addition, the characteristic decay time for the first distribution is much shorter than that for the second distribution.

This work has been financially supported by the Ministry of Education Singapore under Project No. ARC 1/04.

- <sup>1</sup>S. Tiwari, F. Rana, H. Hanafi, A. Hartstein, E. F. Crabbe, and K. Chan, *Appl. Phys. Lett.* **68**, 1377 (1996).
- <sup>2</sup>Y. Shi, K. Saito, H. Ishikuro, and T. Hiramoto, *Jpn. J. Appl. Phys., Part 1* **38**, 2453 (1999).
- <sup>3</sup>R. A. Rao, R. F. Steimle, M. Sadd, C. T. Swift, B. Hradsky, S. Straub, T. Merchant, M. Stoker, S. G. H. Anderson, M. Rossow, J. Yater, B. Acred, K. Harber, E. J. Prinz, B. E. White, Jr., and R. Muralidhar, *Solid-State Electron.* **48**, 1463 (2004).
- <sup>4</sup>Y. Liu, T. P. Chen, C. Y. Ng, M. S. Tse, S. Fung, Y. C. Liu, and S. Li, *Electrochem. Solid-State Lett.* **7**, G134 (2004).
- <sup>5</sup>P. Photopoulos and A. G. Nassiopoulou, *Appl. Phys. Lett.* **77**, 181116 (2000).
- <sup>6</sup>G. Franzò, A. Irrera, E. C. Moreira, M. Miritello, F. Iacona, D. Sanfilippo, G. Di Stefano, P. G. Fallica, and F. Priolo, *Appl. Phys. A: Mater. Sci. Process.* **74**, 1 (2002).
- <sup>7</sup>P. Dimitrakis, E. Kapetanakis, D. Tsoukalas, D. Skarlatos, C. Bonafos, G. B. Assayag, A. Claverie, M. Perego, M. Fanciulli, V. Soncini, R. Sotgiu, A. Agarwal, M. Ameen, C. Sohl, and P. Normand, *Solid-State Electron.* **48**, 1151 (2004).
- <sup>8</sup>C. Y. Ng, T. P. Chen, H. W. Lau, Y. Liu, M. S. Tse, O. K. Tan, and V. S. W. Lim, *Appl. Phys. Lett.* **85**, 2941 (2004).
- <sup>9</sup>C. Guillemot, P. Budau, J. Chevrier, F. Marchi, F. Comin, C. Alandi, F. Bertin, N. Buffet, C. Wyon, and P. Mur, *Europhys. Lett.* **59**, 566 (2002).
- <sup>10</sup>E. A. Boer, L. D. Bell, M. L. Brongersma, H. A. Atwater, M. L. Ostraat, and R. C. Flagan, *Appl. Phys. Lett.* **78**, 3133 (2001).
- <sup>11</sup>E. A. Boer, M. L. Brongersma, H. A. Atwater, R. C. Flagan, and L. D. Bell, *Appl. Phys. Lett.* **79**, 791 (2001).
- <sup>12</sup>D. M. Schaadt, E. T. Yu, S. Sankar, and A. E. Berkowitz, *Appl. Phys. Lett.* **74**, 472 (1999).
- <sup>13</sup>R. M. Nyffenegger, R. M. Penner, and R. Schierle, *Appl. Phys. Lett.* **71**, 1878 (1997).
- <sup>14</sup>T. D. Krauss and L. E. Brus, *Mater. Sci. Eng., B* **69-70**, 289 (2000).